



Title	A nanocarrier system for the delivery of nucleic acids targeted to a pancreatic beta cell line
Author(s)	Yamada, Yuma; Tabata, Mai; Yasuzaki, Yukari; Nomura, Masatoshi; Shibata, Atsushi; Ibayashi, Yuta; Taniguchi, Yosuke; Sasaki, Shigeki; Harashima, Hideyoshi
Citation	Biomaterials, 35(24), 6430-6438 https://doi.org/10.1016/j.biomaterials.2014.04.017
Issue Date	2014-08
Doc URL	http://hdl.handle.net/2115/57456
Type	article (author version)
File Information	WoS_66932_Yamada.pdf



[Instructions for use](#)

A nanocarrier system for the delivery of nucleic acids targeted to a pancreatic beta cell line

Yuma Yamada^a, Mai Tabata^a, Yukari Yasuzaki^a, Masatoshi Nomura^b, Atsushi Shibata^c,
Yuta Ibayashi^b, Yosuke Taniguchi^c, Shigeki Sasaki^c and Hideyoshi Harashima^{a*}

^aLaboratory for molecular design of pharmaceuticals, Faculty of Pharmaceutical Sciences,
Hokkaido University, Kita-12, Nishi-6, Kita-ku, Sapporo 060-0812, Japan

^b Department of Endocrine and Metabolic Diseases / Diabetes Mellitus, Kyushu
University Hospital, 3-1-1 Maidashi, Higashi-ku, Fukuoka 812-8582, Japan

^c Graduate School of Pharmaceutical Sciences, Kyushu University, 3-1-1 Maidashi,
Higashi-ku, Fukuoka 812-8582, Japan

*Corresponding author: Laboratory for molecular design of pharmaceuticals, Faculty of
Pharmaceutical Sciences, Hokkaido University, Kita-12, Nishi-6, Kita-ku, Sapporo 060-
0812, Japan

Tel: +81-11-706-3919 Fax: +81-11-706-4879

E-mail: harasima@pharm.hokudai.ac.jp

Abstract Pancreatic β cells secrete insulin in response to glucose levels and thus are involved in controlling blood glucose levels. A line of pancreatic β cells “MIN6” has been used in studies related to the function of β cells and diabetes therapy. Regulating gene expression in MIN6 cells could accelerate these studies, but an efficient method for the transfection of nucleic acids targeted to MIN6 cells is required. We report here on a liposome-based carrier targeted to pancreatic β cells (Multifunctional envelope-type nano device for pancreatic β cells, β -MEND). We identified a lipid composition for use in preparing the β -MEND, which permits the particles to be efficiently internalized into MIN6, as evidenced by flow cytometry analyses. Intracellular observation by confocal laser scanning microscopy showed that the β -MEND efficiently delivered the oligo nucleic acids to the cytosol of MIN6 cells. Moreover, using a β -MEND encapsulating a 2'-O-Methyl RNA complementary to a microRNA that suppresses insulin secretion, the knockdown of the targeted microRNA and an up-regulation of insulin secretion were observed in MIN6. Thus, the β -MEND holds promise as an efficient system for delivering nucleic acids targeted to MIN6 and can contribute to research and therapy aimed at diabetes.

Key words: MIN6 cell; Nucleic acids delivery; Multifunctional envelope-type nano device (MEND); Pancreatic β cells; Diabetes; microRNA.

1. Introduction

Diabetes mellitus is a multi-factorial disorder characterized by high blood glucose levels, and appears to be caused, in part, by genetic and environmental factors [1, 2]. Mutations of the gene related to pancreatic β cell function have been associated with some types of diabetes mellitus [3, 4]. For example, maturity-onset diabetes of the young (MODY) are caused by mutations in any one of at least six different genes that encode the glycolytic enzyme glucokinase and five transcription factors [5]. These genes are associated with important pancreatic β cell functions, including the production and secretion of insulin which regulates blood glucose levels. Therefore, gene therapy targeted to pancreatic β cells and related studies could be useful for the treatment of many patients suffering from diabetes mellitus.

A line of pancreatic β cells “MIN6” has been established from mouse insulinomas, and has morphological characteristics that are similar to those of pancreatic β cells. In addition, MIN6 cells exhibit glucose-inducible insulin secretion comparable to that of cultured normal mouse islet cells [6]. Thus, the MIN6 cell line is useful in studies of the molecular mechanisms of pancreatic β cells, and has been used in research directed to the study of the pancreatic β cells function and diabetes therapy [7-9]. The regulation of gene expression in MIN6 cells could accelerate these studies, but an efficient method

for the transfection of nucleic acids targeted to MIN6 cells is required. To date, while the transfection of nucleic acids into MIN6 cells using a viral vector [9] and electroporation [8] has been achieved, the transfection efficiency does not appear to be sufficient. Considering such a situation, a nanocarrier system capable of delivering nucleic acids targeted to MIN6 cells is essential for future research on the function of β cells and diabetes therapy.

In previous studies, we reported on the development of a multifunctional envelope-type nano device (MEND), which consists of a condensed plasmid DNA (pDNA) core and lipid envelopes [10, 11], which showed transfection activities as high as that for a viral vector in dividing cells [12]. To date, we have been successful in efficiently packaging nucleic acids, including oligo DNA [13, 14] and siRNA [15, 16], and showed that the MEND system achieved efficient gene silencing and RNA knockdown [14-19]. These results prompted us to consider the possibility that a MEND system could be used to achieve the efficient cytosolic delivery of nucleic acids targeted to impregnable MIN6 cells.

In this study, we report on our attempts to develop β -MEND, which is a MEND that permits the efficient delivery of nucleic acids to pancreatic β cells. We conclude that the β -MEND reported on here, constitutes a breakthrough in research on the function of

β cells and diabetes therapy. We first identified a lipid composition for the β -MEND that permits it to be efficiently internalized into MIN6 cells. This was achieved by varying the lipid composition of a panel of liposomes (LPs) labelled with fluorescent lipids and cellular uptake analysis by flow cytometry. We next constructed the β -MEND in which nucleic acids were encapsulated, and the fluorescent labeled nucleic acids that were internalized in MIN6 by the β -MEND were measured by flow cytometry. We also observed the intracellular trafficking of the nucleic acids using confocal laser scanning microscopy (CLSM). Moreover, when a β -MEND encapsulating a 2'-O-Methyl (2'-OMe) RNA which targets a microRNA (miRNA) that suppresses insulin secretion was used, the knockdown of the targeted miRNA and the up-regulation of insulin secretion were observed and evaluated in MIN6 cells.

2. Materials and methods

2.1. Materials

1,2-dioleoyl-sn-glycero-3-phosphocholine (DOPC), 1,2-dilawroyl-sn-glycero-3-phosphocholine (DLPC), 1,2-dimyristoyl-sn-glycero-3-phosphocholine (DMPC), 1,2-dipalmitoyl-sn-glycero-3-phosphocholine (DPPC), egg yolk phosphatidyl choline (EPC), 1-palmitoyl-2-oleoyl-sn-glycero-3-phosphocholine (POPC) and 1-stearoyl-2-oleoyl-sn-glycero-3-phosphocholine (SOPC) were obtained from Nippon Oil and Fats Co. (Tokyo, Japan). Cardiolipin (CL), cholesteryl hemisuccinate (CHEMS), phosphatidic acid (PA) and phosphatidyl glycerol (PG) were purchased from Sigma (St. Louis, MO, USA). Cholesterol (Chol), 3 β -[N-(N',N'-dimethylaminoethane)-carbamoyl] cholesterol (DC-Chol), dimethyldioctadecylammonium bromide (DDAB), 1, 2-dioleoyl-sn-glycero-3-phosphatidyl ethanolamine (DOPE), 1,2-dioleoyl-3-trimethylammonium-propane (DOTAP), 1,2-di-O-octadecenyl-3-trimethylammonium propane (DOTMA), 1-stearoyl-2-oleoyl-sn-glycero-3-phosphoethanolamine (SOPE) and sphingomyelin (SM) were purchased from Avanti Polar lipids (Alabaster, AL, USA). Stearyl octaarginine (STR-R8) [20] was obtained from KURABO Industries Ltd (Osaka, Japan). The oligo DNA (5'-CTTCTCGTCCCCATGGATGACCCC-3') and the oligo DNA labeled with fluorescent that Cy5 is conjugated to 5 terminal of the oligo DNA were obtained from Hokkaido

System Science Co., Ltd (Sapporo, Japan). 2'-OMe RNA complementary to miR-375 (anti-miR-375) (5'-UGCAUCACGCGAGCCGAACGAACAAAUAAG) and antisense 2'-OMe RNA targeting green fluorescent protein (control RNA) (AAGGCAAGCUGACCCUGAAGU) were obtained from Greiner Japan (Tokyo, Japan). Protamine was purchased from CALBIO CHEM (Darmstadt, Germany). HeLa human cervix carcinoma cells were obtained from the RIKEN Cell Bank (Tsukuba, Japan). MIN6 cells, a mouse pancreatic beta cell line [6], were generously provided by Dr. J. Miyazaki (Osaka University, Japan). Dulbecco's modified Eagle medium (DMEM), fetal bovine serum (FBS), Lipofectamine Plus (LFN Plus) and tetramethylrhodamine (TMRM) were purchased from Life Technologies Corporation (Carlsbad, CA, USA). All other chemicals used were commercially available reagent-grade products.

2.2. Cell culture and transfection studies

HeLa cells were cultured in DMEM supplemented with 10% FBS and penicillin (100 U/mL), streptomycin (100 µg/mL) under an atmosphere of 5% CO₂ at 37°C. MIN6 cells were cultured in DMEM containing 25 mM glucose and supplemented with 10% FBS and penicillin (100 U/mL), streptomycin (50 µg /mL) under an atmosphere of 5% CO₂ at 37°C. MIN6 cells (4 x 10⁵ cells/mL) or HeLa cells (1 x 10⁵ cells/mL) were seeded

with DMEM containing 10% FBS, on a 12 well plate (Corning, NY, USA; DMEM volume, 1 mL) for flow cytometry analysis and a 35 mm glass base dish (IWAKI, Tokyo, Japan; DMEM volume, 2 mL) for confocal laser scanning microscopy (CLSM). Moreover, MIN6 cells (4×10^5 cells/mL) were seeded with DMEM containing 10% FBS, on a 24 well plate (Corning; DMEM volume, 500 μ L) for insulin secretion studies, a 12 well plate (Corning; DMEM volume, 1 mL) for cytotoxicity evaluation and reverse transcription and polymerase chain reaction (RT-PCR).

2.3. Preparation of NBD-labeled LPs

LPs were prepared by the lipid hydration method. A lipid film containing 0.5 mol% 7-nitrobenz-2-oxa-1, 3-diazole labelled DOPE (NBD-DOPE) (Avanti Polar lipids) was prepared on the bottom of a glass tube by evaporation of an ethanol solution containing 150 nmol lipids, as shown in [Table 1](#). Next, 250 μ L of 10 mM 4-(2-hydroxyethyl)-1-piperazineethanesulfonic acid (HEPES) buffer (pH 7.4) was applied to the lipid film, followed by incubation for 15 min at room temperature. The lipid film was then sonicated for 30 sec in a bath-type sonicator (85 W, Aiwa Co., Tokyo, Japan). R8-modified LP (R8-LP) was prepared by mixing the LP (DOPE/PA = 9:2, molar ratio) suspensions and an STR-R8 solution (10 mol% of lipid).

2.4. Preparation of MEND encapsulating Cy5-labeled oligo DNA

Negatively charged nanoparticles of oligo DNA (final oligo DNA concentration, 61.5 $\mu\text{g/mL}$) were prepared as follows; a solution of oligo DNA was added to the protamine solution under vortexing at a nitrogen/phosphate (N/P) ratio of 1.0 for β -MEND (DC-Chol/EPC/SM = 3:4:3, molar ratio). While a solution of oligo DNA was added to the STR-R8 solution under vortexing at an N/P ratio of 3.0 in the case of the preparation of positively charged nanoparticles for the R8-MEND (DOPE/PA/STR-R8 = 9:2:1, molar ratio). A lipid film was prepared by the evaporation of a chloroform solution of 825 nmol lipid [(DC-Chol/EPC/SM = 3:4:3, molar ratio) or (DOPE/PA = 9:2, molar ratio)] on the bottom of a glass tube, followed by hydration with 1.5 mL of 10 mM HEPES buffer (pH 7.4) for 15 min at room temperature. The glass tube was sonicated in a bath-type sonicator (AU-25C; Aiwa Co.), followed by sonication for 10 min in ice-cold water with a probe-type sonicator (Digital Sonifier 250; Branson Ultrasonics Co., Danbury, CT, USA) to produce small unilamellar vesicle (SUV). β -MEND was constructed by mixing negatively charged oligo DNA nanoparticles and with twice the volume of positively charged SUV (DC-Chol/EPC/SM = 3:4:3, molar ratio) suspension. For the preparation of R8-modified MEND (R8-MEND), positively charged oligo DNA nanoparticles were

mixed with twice the volume of negatively charged SUV (DOPE/PA = 9:2, molar ratio) suspension, followed by incubation with STR-R8 (10mol% of total lipids) for 30 min at room temperature.

2.5. Preparation of β -MEND encapsulating 2'-OMe RNA

A solution of 2'-OMe RNA was added to the protamine solution under vortexing at an N/P ratio of 1.0. A lipid film was prepared on the bottom of a glass tube by evaporation of an ethanol solution containing 150 nmol lipids (DC-Chol/EPC/SM = 3:4:3, molar ratio). 250 μ L of a solution of 2'-OMe RNA nanoparticles was applied to the lipid film, followed by incubation for 15 min at room temperature. The lipid film was then sonicated for 30 sec in a bath-type sonicator (85 W, Aiwa Co.).

2.6. Characterization of prepared carriers

Particle diameters were measured using a dynamic light scattering (DLS) method (Zetasizer Nano ZS; Malvern Instruments, Worcestershire, UK). Samples were prepared in 10 mM HEPES buffer at 25°C and the values are shown in the form of volume distribution. The ξ -potentials of samples were also determined in 10 mM HEPES buffer at 25°C using a Zetasizer Nano ZS. The encapsulation efficiency of nucleic acids (oligo

DNA or 2'-OMe RNA) was determined using a fluorescent nucleic acid stain for quantitating nucleic acids, RiboGreen dye (Life Technologies Corporation) [21], as previously reported [17].

2.7. Quantification of the cellular uptake using flow cytometry

Cells were washed with serum-free DMEM before incubation with the carriers. The carriers with lipid envelopes labeled with 1 mol% NBD-DOPE were added to the cells (final lipid concentration, 27.5 μ M) for the experiment shown in [Figure 1A](#) and [2](#). While the carriers with 5 mol% Cy5 labeled oligo DNA were used in [Figure 3A](#) (final concentration of oligo DNA, 25-200 nM) and [Figure 4](#) (final concentration of oligo DNA, 100 nM). The cells were then incubated in serum-free medium for 1 hr or 3 hr under an atmosphere of 5% CO₂ at 37°C. After removing the medium, the cells were washed once with ice-cold phosphate-buffered saline (PBS (-)) and twice with ice-cold PBS (-) containing heparin (20 U/mL). The cells were trypsinized and then suspended in DMEM with serum. After centrifugation (700g, 4°C, 3 min), the supernatant was removed and cells were resuspended in 0.5 mL of PBS (-) containing 0.5% bovine serum albumin (BSA) and 0.1% NaN₃. The cell suspension was filtered through a nylon mesh followed by analysis by flow cytometry (FACScan, Becton Dickinson, Franklin Lakes, NJ, USA).

NBD or Cy5 was excited at 488 nm, 633 nm light and fluorescence detection channel was set to FL1 filter for NBD, FL4 filter for Cy5. The cellular uptake was expressed as mean fluorescence intensity (MFI), calculated using the CellQuest software (Becton Dickinson, Franklin Lakes, NJ, USA).

To investigate the mechanism of the cellular uptake of carriers, the cells were treated with inhibitors (0.3 M sucrose, 5 mM amiloride, or 2 μ M filipin) for 30 min before addition of the carriers into the cells. Relative cellular uptake when the cells were treated with inhibitors was calculated as follows;

$$\text{Relative cellular uptake value (\%)} = U_P/U_A \times 100$$

where U_P and U_A represent the cellular uptake when cells were treated with carriers in the presence and absence of inhibitors, respectively.

2.8. Visualization of intracellular oligo DNAs by CLSM

Cells were washed with serum-free DMEM before incubation with the carriers. The carriers in which the lipid envelopes were labeled with 1 mol% NBD-DOPE were added to the cells (final lipid concentration, 14.2 μ M) for the experiment shown in [Figure 1B](#). While the carriers with 5 mol% Cy5 labeled oligo DNA were used in [Figure 3B](#) (final concentration of oligo DNA, 100 nM). The cells were then incubated in serum-free

DMEM under an atmosphere of 5% CO₂ at 37°C. After a 3-hr incubation, the cells were observed by CLSM (FV 10i-LIV, OLYMPUS, Tokyo, Japan) after staining the nuclei or mitochondria. In the case of nuclei staining, 10 minutes before the acquisition of fluorescence images, Hoechst33342 (DOJINDO Laboratories, Kumamoto, Japan) was added to the medium with serum at a final concentration of 5 µg/mL. In the case of mitochondrial staining, 45 minutes before the acquisition of the fluorescence images, the medium was replaced with fresh medium containing TMRM (final concentration, 50 nM) and the cells were incubated in this solution.

After the staining procedure, the cells were washed with medium containing serum, and then observed by CLSM in the same medium. The cells were excited with a 405 nm light for detecting Hoechst33342, 473 nm light for detecting NBD-DOPE, 559 nm light for detecting TMRM and a 635 nm light for detecting Cy5 from a LD laser. Images were obtained using an FV10i-LIV equipped with a water-immersion objective lens (UPlanSApo 60x/NA = 1.2) and a dichroic mirror (DM405/473/559/635). The fluorescence detection channels (Ch) were set to the following filters: Ch1: BP 420-460 (cyan color) for Hoechst 33342, Ch2: BP 490-540 (green color) for NBD-DOPE, Ch3: BP 570-620 (red color) for TMRM and Ch4: BP 660-710 (green pseudo color) for Cy5.

2.9. Evaluation for cytotoxicity

Cells were washed with serum-free DMEM before being incubated with the carriers. The carriers encapsulating oligo DNA were added to the cells (final concentration of oligo DNA, 25 - 400 nM), and the cells incubated in serum-free DMEM under an atmosphere of 5% CO₂ at 37°C. After a 3-hr incubation, the medium was replaced with medium containing serum, and the cells further were incubated for 21 hr. The cells were then washed, and the cellular protein content was determined using a BCA protein assay kit (PIERCE; Rockford, IL, USA) and an EnSpire™ 2300 Multilabel Reader (PerkinElmer, Inc.; Waltham, MA, USA). Cell viability was calculated as follows;

$$\text{Cell viability (\%)} = C_S/C_N \times 100$$

where C_S and C_N represent the cellular protein concentration when cells were treated with carriers encapsulating oligo DNA and non-treated cells, respectively.

2.10. RNA extraction and RT-PCR after transfection of 2'-OMe RNA into MIN6 cells

Cells were washed with serum-free DMEM before incubation with the carriers. The carriers encapsulating 2'-OMe RNA (anti-miR-375) were added to the cells (final concentration of 2'-OMe RNA, 0.1 - 50 nM), and the cells incubated in serum-free DMEM under an atmosphere of 5% CO₂ at 37°C. After a 3-hr incubation, the medium

was replaced with medium containing serum, and the cells were incubated for a further 21 hr.

After incubation, the cells were washed three times with PBS (-), total RNA was then extracted using TRIzol reagent (Life Technologies Corporation) according to the manufacturer's protocols. Reverse transcription was performed with 500 ng of total RNA using TaqMan reverse transcription kit (Life Technologies Corporation) according to the manufacturer's protocols. Each of the mRNA transcripts was subjected to quantitative PCR with TaqMan MicroRNA Assays (Life Technologies Corporation) and an ABI 7500 real-time system to determine the quantities of miRNA coding miR-375 [target sequence] and snoRNA234 [control sequence]. After an enzyme activation step for 10 min at 95°C, the DNA was denatured at 95°C for 15 sec, and annealing/extension was performed at 60°C for 1 min. The denaturation/annealing cycle was repeated 40 times.

Briefly, we normalized each set of samples using the difference in threshold cycles (ΔC_T) between the target miRNA (miR-375) and the housekeeping gene (snoRNA234): $\Delta C_T = (\Delta C_{T \text{ miR-375}} - \Delta C_{T \text{ snoRNA-234}})$. The calibrator sample ($\Delta C_{T \text{ calibration}}$) was assigned as the sample with non-treated cells. The relative miR-375 expression levels were calculated by the expression $2^{-\Delta\Delta C_T}$ where $\Delta\Delta C_T = \Delta C_{T \text{ miR-375}}(n) - \Delta C_{T \text{ calibration}}(n)$. Each reaction was done, at least in duplicate.

2.11. Insulin secretion studies

Cells were washed with serum-free DMEM before incubation with the carriers. The carriers encapsulating 2'-OMe RNA (anti-miR-375 or control RNA) were added to the cells (final concentration of 2'-OMe RNA, 10 - 100 nM), and the cells were then incubated in serum-free DMEM under an atmosphere of 5% CO₂ at 37°C. After a 3-hr incubation, the medium was replaced with medium containing serum, and the cells were incubated for a further 45 hr. After this incubation, the cells were washed once with PBS (-), and incubated with HEPES-added Krebs-Ringer Bicarbonate buffer containing 0.5% BSA (HKRB [BSA] buffer) containing 3 mM glucose for 30 min. The cells were then washed twice with PBS (-), followed by incubation with HKRB [BSA] buffer with 30 mM glucose for 1 hr. The supernatant of the medium was collected, the insulin secretion of the samples was measured using Ultra Sensitive Rat Insulin ELISA Kit (Morinaga, Kanagawa, Japan) and an EnSpire™ 2300 Multilabel Reader (PerkinElmer, Inc.). Each reaction was performed, at least in duplicate. Insulin secretion was calculated as follows;

$$\text{Relative insulin secretion (\%)} = C_A/C_C \times 100$$

where C_A and C_C represent the insulin concentration of the medium when cells were treated with carriers encapsulating anti-miR-375 and control RNA, respectively.

2.12. Statistical analysis

Data are expressed as the mean \pm S.D. for the indicated number of experiments.

For comparison between two groups, the two tail unpaired student's t-test was used. For multiple comparisons, one way ANOVA was used. $P < 0.05$ was considered to be statistically significant.

3. Results

3.1. Screening for a lipid composition with high affinity to MIN6 cells

We recently developed a MEND, consisting of a condensed pDNA core and lipid envelopes [10, 11], the surface of which was modified with high-density R8, an artificially designed cell penetrating peptide [20, 22], to produce the R8-MNED. A previous report showed that high-density R8-modified carriers were internalized primarily via macropinocytosis rather than clathrin-mediated endocytosis, as is the case of cationic LPs [23, 24]. Moreover, the R8-MEND showed transfection activities in dividing cells that were as high as that for adenovirus [12]. Based on these results, we predicted that the R8-MEND would be efficiently taken up by cells, even MIN6 cells.

To validate this issue, we evaluated the cellular uptake of R8-LP using MIN6 cells and HeLa cells, which was efficiently internalized by R8-modified carriers [12]. The diameter and ζ -potential of R8-LP (10 mol% R8 of lipids) used in this experiment were ~ 130 nm and $\sim +50$ mV (Table S1). Flow cytometry analyses indicated a low cellular uptake of R8-LPs in the case of MIN6 cells (Fig. 1A (a)). The fluorescence intensities of R8-LPs labeled with NBD-lipids taken up by cells (pink line) were comparable with that of non-treated cells (black line), although the value for the R8-LPs (pink line) was slightly increased compared to R8-unmodified LPs (green line). On the other hand, in the case

of HeLa cells (Fig. 1A (b)), cellular uptake for the R8-LPs was much higher than that of the R8-unmodified LPs and non-treated cells. The cellular uptake values (MFI) of R8-LPs in the case of MIN6 cells and HeLa cells were ~ 7 and ~ 95 , respectively (Figs. S1, S2). Intracellular observation of the R8-LPs also showed that no R8-LPs were observed in MIN6 cells (Fig. 1B (a)), while, green signals corresponding to R8-LPs labeled with NBD-lipids were observed in HeLa cells (Fig. 1B (b)).

We screened for an LP that is efficiently internalized into MIN6 cells by varying the lipid composition of the LPs. Table 1 summarizes the lipid compositions of LPs prepared in this screening, their diameters and ζ potentials. These LPs were labeled with NBD-lipids and incubated with MIN6 cells, and cellular uptake efficiency was investigated by measuring the fluorescence of the LPs taken up by MIN6 cells using flow cytometry. We first investigated the cellular uptake of A-type LPs (DOTAP/EPC/Lipid X = 3:4:3, molar ratio) (Fig. 2A). As a result, it was observed that the cellular uptake of positively charged LPs containing CL, Chol and SM were higher than that for negatively charged LPs containing PG, CHEMS and PA. In the case of A-type LPs, an SM containing LP showed the highest cellular uptake. We then evaluated the cellular uptake of B-type LPs (Lipid X/EPC/SM = 3:4:3, molar ratio), which were SM-containing LPs composed of different types of cationic lipids (Table 1). The results showed that the value

for the cellular uptake of a DC-Chol containing LP was the highest among the B-type LPs (Fig. 2B), suggesting that DC-Chol is an optimal cationic lipid for the efficient internalization of LP by MIN6 cells. Finally, we investigated the cellular uptake of C-type LPs (DC-Chol/Lipid X/SM = 3:4:3, molar ratio), which were positively charged LPs containing DC-Chol and SM (Table 1). The cellular uptake efficiencies of the LPs were comparable (Fig. 2C), as a result, EPC containing C-type LPs exhibited the highest cellular uptake efficiency among all of the LPs examined. Based on these results, we used the lipid composition: DC-Chol/EPC/SM = 3:4:3, molar ratio for preparing the β -MEND, which has a high affinity for MIN6 cells, model pancreatic β cells.

3.2. Evaluation of the cellular uptake efficiency of β -MEND and intracellular observation of encapsulated nucleic acids in MIN6

We constructed a β -MEND encapsulating nucleic acids (Cy5 labelled oligo DNA) and evaluated the cellular uptake efficiency of this β -MEND using flow cytometry. For the β -MEND, the envelope was comprised of the high affinity lipid composition for internalization by MIN6 cells (DC-Chol/EPC/SM = 3:4:3, molar ratio), while an R8-MEND, composed of the lipid composition (DOPE/PA/STR-R8 (9:2:1, molar ratio)) required for achieving efficient cytosolic delivery in HeLa cells, NIH3T3 cells and related

cell lines [25, 26], was prepared as the control carrier. The characteristics of the carriers are summarized in [Table 2](#). Their ζ -potentials were around + 25 mV and the encapsulation efficiencies were around 50%.

Flow cytometry analyses showed that β -MEND resulted in a more efficient internalization of oligo DNA into MIN6 cells than the R8-MEND and LFN Plus, a commercially available transfection reagent ([Fig. 3A](#)). It was also confirmed that the introduction of oligo DNA by the β -MEND was proportional to the applied dose, while those by R8-MEND and LFN Plus were saturated. Moreover, intracellular observations by CLSM provided us with information regarding the intracellular fate of oligo DNA after transfection by these carriers ([Fig. 3B](#)). In the case of the β -MEND, many green fluorescence signals derived from Cy5 labelled oligo DNA were distributed in the cytosol of MIN6 cells ([Fig. 3B \(a\)](#)). On the other hand, only a few green dots were localized within the cells in the case of the R8-MEND and LFN Plus ([Fig. 3B \(b\), \(c\)](#)). Based on these results, it was concluded that the β -MEND could achieved efficient cytosolic delivery of nucleic acids into MIN6 cells.

3.3. Analysis for the cellular uptake route of β -MEND into MIN6 cells and the evaluation of the cell viability

To investigate the contribution of the cellular uptake pathway in the internalization of the carriers, we transfected Cy5 labelled oligo DNA into MIN6 cells using β -MEND, R8-MEND and LFN Plus in the presence or absence of specific inhibitors of each type, and then measured the internalized oligo DNA by flow cytometry (Fig. 4). Clathrin-mediated endocytosis is the major and best characterized endocytic pathway, and macropinocytosis and caveolae uptake represent other types of cellular uptake pathways [27, 28]. We examined the effects of the following inhibitors: a hypertonic medium to specifically inhibit clathrin-mediated endocytosis through dissociation of the clathrin lattice, amiloride to specifically inhibit macropinocytosis by inhibiting the Na/H exchange required for macropinocytosis, and filipin to specifically inhibit caveolar uptake through cholesterol depletion [27, 28].

As shown in Figure 4A, the use of a hypertonic medium containing sucrose specifically inhibited clathrin-mediated uptake of all types of carriers by 50%. In the presence of the macropinocytosis inhibitor (amiloride), the cellular uptake of carriers was inhibited in the case of both β -MEND and R8-MEND, whereas no inhibition of the cellular uptake was observed in the case of LFN Plus (Fig. 4B). The inhibitor of caveolar uptake (filipin) inhibited the uptake of the R8-MEND, while both the β -MEND and LFN Plus were internalized (Fig. 4C). Taken together, these results indicate that the β -MEND

involves classic clathrin-mediated endocytosis and macropinocytosis, whereas the R8-MEND utilizes all uptake pathways examined in this experiment. In the case of LFN Plus, cellular uptake would involve clathrin-mediated endocytosis as a major uptake pathway.

We also evaluated the cell viabilities of these carriers based on protein contents using MIN6 cells. As shown in [Figure 5](#), none of the carriers showed any cell toxicity in the case of a low applied dose. Moreover, the β -MEND and LFN Plus had no toxicity, even at a high applied dose, while the R8-MEND had a slight toxicity at an applied dose higher than 200 nM of oligo DNA concentration.

3.4. Evaluation of miR-375 knockdown by 2'-OMe RNA (anti-miR-375) delivery targeted to MIN6 using β -MEND

We attempted the knockdown of an miRNA involved in the regulation of insulin secretion (miR-375) by transfection of the anti-miR-375 into MIN6 cells using β -MEND. It is known that miR-375 is highly expressed in pancreatic β cells, and inhibits protein expression of the phosphoinositide-dependent protein kinase 1 (Pdk1) [29] and myotrophin (Mtpn) [30], which activate insulin secretion in response to the surrounding glucose concentration. Thus, it would be predicted that the knockdown of the miR-375 would increase the expression levels of Pdk1 and Mtpn to activate the insulin secretion.

We packaged anti-miR-375 in the β -MEND, and attempted the knockdown of miR-375 in MIN6 cells by the β -MEND system. The diameter and ζ -potential of the β -MENDs were 174 ± 35 nm and 45 ± 5 mV, respectively (n=7-9). The encapsulation efficiency of the 2'-OMe RNA was $63 \pm 9\%$ (n=3).

After a 24 hr transfection of anti-miR-375 into MIN6 cells by the β -MEND, quantitative RT-PCR was performed to evaluate the extent of knockdown of miR-375. [Figure 6](#) provides information on the transfection concentration of anti-miR-375 (x-axis) and the relative miR-375 expression level (y-axis). The results showed that more than a 90% knockdown of miR-375 occurred when the transfection of anti-miR-375 was performed at a concentration of 10 nM by the β -MEND system. It was also confirmed that the β -MEND could achieve a more efficient knockdown of miR-375 compared to LFN Plus, a commercially available transfection reagent. Moreover, western blotting analysis indicated that the expression levels of Pdk1 and Mtpn increased, when the knockdown of miR-375 was performed using the β -MEND system ([Fig. S3](#)).

3.5. Assessment of insulin secretion in response to the surrounding glucose concentration after knockdown of miR-375 by β -MEND system

To evaluate insulin secretion in response to the surrounding glucose

concentration after the knockdown of miR-375, we measured the levels of insulin secretion by ELISA analysis (Fig. 7). In this experiment, MIN6 cells were transfected with anti-miR-375 at 10, 50 and 100 nM concentrations using β -MEND or LFN Plus, and the glucose induced insulin secretion was assessed at 48 hr after the transfection. Using the β -MEND system, the insulin levels were increased when anti-miR-375 was transfected at 50 and 100 nM. While, the effect of anti-miR-375 transfection using LFN Plus on insulin levels was negligible at all concentrations examined. It was also confirmed that the insulin levels were found to be significantly increased by the β -MEND system compared to LFN Plus.

4. Discussion

In this study, we report on attempts to develop a nucleic acid carrier consisting of a unique lipid envelope (referred to herein as a "β-MEND") targeted to MIN6 cells. The MIN6 cell line has been used in research on the function of β cells and diabetes therapy [7-9], thus a nucleic acid delivery system targeted to MIN6 cells could accelerate our understanding in these fields. We focused on the development of a non-viral vector, R8-MEND [10, 11] with a high transfection activity similar to that of adenovirus [12], efficiently packaging nucleic acids such as oligo DNA and siRNA [13-16]. Unexpectedly, flow cytometry analyses and intracellular observations indicated that an efficient cellular uptake of R8-modified carriers (DOPE/PA/STR-R8 = 9:2:1, molar ratio) could not be achieved in the case of MIN6 cells, as shown in [Figure 1](#).

These experiments did, however, provide us with information showing that the R8-modification on the surface of LPs slightly enhanced cellular uptake in MIN6 cells, suggesting that positively charge particles would be required for the high affinity lipid composition with MIN6 cells. Moreover, we investigated cellular uptake using LPs modified with various amounts of R8 ([Fig. S1](#), [Table S1](#)). The ζ-potentials of the R8-LPs increased and were saturated at + 60 mV ([Table S1](#)), and cellular uptake increased as a function of the amount of R8-modification on the surface of the LPs ([Fig. S1](#)). However,

cellular uptake was not drastically increased. In the case of R8-modified carriers, the low cellular uptake in MIN6 cells might be the result of cytotoxicity, as shown in [Figure 5](#). Thus, we screened a lipid composition for use in preparing the β -MEND using various cationic LPs without R8.

In the case of A-type LPs (DOTAP/EPC/Lipid X = 3:4:3, molar ratio) ([Table 1](#)), the cellular uptake of positively charged LPs was higher than that of negatively charged LPs ([Fig. 2A](#)). SM, a neutral lipid, contributes to the formation of LPs with high positively charged LPs ([Table 1](#)) and the SM containing LP showed the highest cellular uptake. It was presumed that SM might efficiently display a positive charge on the surface of the LPs. We then screened a series of cationic lipids to identify a lipid composition for an SM containing LP using B-type LPs (Lipid X/EPC/SM = 3:4:3, molar ratio) ([Table 1](#)). As a result, the cellular uptake for the DC-Chol containing LP was the highest among the B-type LPs (cellular uptake, around 60 MFI; ξ -potential, around +60 mV) ([Fig. 2B](#)), although the DOTMA containing LP had the highest positive charge (cellular uptake, around 40 MFI; ξ -potential, around +70 mV) ([Table 1](#)). While, DDAB containing LP and R8-LP with a positive charge similar to that for DC-Chol containing LP (ξ -potential, +50–60 mV) showed the low cellular uptake in MIN6 cells (less than 20 MFI). These results suggest that a high affinity lipid composition with MIN6 cells would require an optimal

positive charge and other factors. Finally, we selected an optimal main component, namely, phosphatidylcholine (PC) and phosphatidylethanolamine (PE), a neutral lipid widely used for preparation of LPs using C-type LPs (DC-Chol/Lipid X/SM = 3:4:3, molar ratio) (Table 1). The cellular uptake efficiencies of the LPs were comparable (Fig. 2C), and EPC containing C-type LPs (DC-Chol/EPC/SM = 3:4:3, molar ratio) exhibited the highest cellular uptake efficiency among all of the LPs examined (Fig. 2).

We succeeded in constructing a β -MEND (DC-Chol/EPC/SM = 3:4:3, molar ratio) encapsulating nucleic acids, and found that its use resulted in a dramatic improvement of transfection efficiency of nucleic acids by the β -MEND system compared with the R8-MEND or LFN Plus (Figs 3). However, the specific reason for why the lipid composition of the β -MEND is optimal for cellular uptake in MIN6 cells was unknown. Thus, we validated route for the cellular uptake of the β -MEND in MIN6 cells to obtain a clue to this issue. As shown in Figure 4, the β -MEND involves classic clathrin-mediated endocytosis and macropinocytosis, whereas LFN Plus involves clathrin-mediated endocytosis as a major uptake pathway. The results indicate that macropinocytosis contributes to the high cellular uptake of β -MEND in MIN6 cells, however, this hypothesis cannot be used to explain the following result. The cellular uptake of R8-MEND by MIN6 cells was significantly lower than that for the β -MEND (Fig. 3),

although the R8-MEND involves classic clathrin-mediated endocytosis, macropinocytosis and the caveolar pathway (Fig. 4). In some pathways, the cellular uptake process involves carriers binding to the cellular surface, followed by internalization into the interior of cells. One possibility is that the high cellular uptake of the β -MEND by MIN6 cells might be mainly contributed by efficient binding to the cell rather than the internalization process. Another possibility is that β -MEND might be internalized into the interior of cells via an as-yet unknown pathway, which contributes to the high cellular uptake of the β -MEND in MIN6 cells.

As shown in Figure 6, the β -MEND system resulted in the efficient knockdown of the targeted miR-375 when 10 nM of anti-miR-375 was transfected, while the up-regulation of insulin secretion was observed for a transfection of more than 50 nM of anti-miR-375 (Fig. 7). It is likely that many factors are involved in the regulation of the insulin secretion in MIN6, thus regulation might not be achieved by only the knockdown of the miR-375, although more than a 90% knockdown occurred in the case of a transfection of 10 nM of anti-miR-375. In contrast, in the case of an anti-miR-375 transfection of more than 50 nM, other factors including functional molecules, cell signaling, external conditions might be adjusted to achieve optimal conditions for insulin secretion.

5. Conclusion

In this study, we successfully identified a lipid composition (DC-Chol/EPC/SM = 3:4:3, molar ratio) for the β -MEND that comprised a high affinity envelope for MIN6 cells, model pancreatic β cells. Flow cytometry analysis and intracellular observations by CLSM indicated that the β -MEND efficiently delivered nucleic acids to the cytosol in MIN6 cells. Moreover, the transfection of 2'-OMe RNA complementary to miR-375 into MIN6 cells by the β -MEND system resulted in the efficient knockdown of the targeted miRNA and regulation of cellular functions that are related to insulin secretion. The findings that the β -MEND was a noninvasive device and that it regulated cell function indicates that this nanocarrier system could be used in clinical applications. These results suggest that the β -MEND holds promise as an efficient delivery system for nucleic acids targeted to MIN6 and can contribute to research and therapy aimed at diabetes.

Acknowledgements

This work was supported, in part by, the Program for Promotion of Fundamental Studies in Health Sciences of the National Institute of Biomedical Innovation, Japan (NIBIO), a Grant-in-Aid for Scientific Research (S) from the Ministry of Education, Culture, Sports, Science and Technology of Japanese Government (MEXT). We thank Dr. J. Miyazaki for providing MIN6 cells. We also thank Dr. Milton Feather for his helpful advice in writing the manuscript.

References

1. Eckel RH, Grundy SM, Zimmet PZ. The metabolic syndrome. *Lancet*. 2005;365:9468:1415-28.
2. Tusie Luna MT. Genes and type 2 diabetes mellitus. *Arch. Med. Res.* 2005;363:210-22.
3. Pearson ER. Recent advances in the genetics of diabetes. *Prim. care diabetes*. 2008;22:67-72.
4. Bell GI, Polonsky KS. Diabetes mellitus and genetically programmed defects in beta-cell function. *Nature*. 2001;414:6865:788-91.
5. Stride A, Hattersley AT. Different genes, different diabetes: lessons from maturity-onset diabetes of the young. *Ann. Med.* 2002;343:207-16.
6. Miyazaki J, Araki K, Yamato E, Ikegami H, Asano T, Shibasaki Y, et al. Establishment of a pancreatic beta cell line that retains glucose-inducible insulin secretion: special reference to expression of glucose transporter isoforms. *Endocrinology*. 1990;127:126-32.
7. Tersey SA, Nishiki Y, Templin AT, Cabrera SM, Stull ND, Colvin SC, et al. Islet beta-cell endoplasmic reticulum stress precedes the onset of type 1 diabetes in the nonobese diabetic mouse model. *Diabetes*. 2012;614:818-27.
8. Geisler JC, Corbin KL, Li Q, Feranchak AP, Nunemaker CS, Li C. Vesicular nucleotide transporter-mediated ATP release regulates insulin secretion. *Endocrinology*. 2013;154:675-84.
9. de Azua IR, Scarselli M, Rosemond E, Gautam D, Jou W, Gavrilova O, et al. RGS4 is a negative regulator of insulin release from pancreatic beta-cells in vitro and in vivo. *Proc. Natl. Acad. Sci. U.S.A.* 2010;107:7999-8004.
10. Kogure K, Moriguchi R, Sasaki K, Ueno M, Futaki S, Harashima H. Development of a non-viral multifunctional envelope-type nano device by a novel lipid film hydration method. *J. Control. Release*. 2004;98:317-23.
11. Nakamura T, Akita H, Yamada Y, Hatakeyama H, Harashima H. A multifunctional envelope-type nanodevice for use in nanomedicine: concept and applications. *Acc. Chem. Res.* 2012;45:1113-21.
12. Khalil IA, Kogure K, Futaki S, Hama S, Akita H, Ueno M, et al. Octaarginine-modified multifunctional envelope-type nanoparticles for gene delivery. *Gene Ther.* 2007;14:682-9.
13. Yamada Y, Kogure K, Nakamura Y, Inoue K, Akita H, Nagatsugi F, et al. Development of efficient packaging method of oligodeoxynucleotides by a condensed nano particle in lipid envelope structure. *Biol. Pharm. Bull.* 2005;28:1939-42.
14. Nakamura Y, Kogure K, Yamada Y, Futaki S, Harashima H. Significant and prolonged antisense effect of a multifunctional envelope-type nano device encapsulating antisense oligodeoxynucleotide. *J. Pharm. Pharmacol.* 2006;58:431-7.

15. Nakamura Y, Kogure K, Futaki S, Harashima H. Octaarginine-modified multifunctional envelope-type nano device for siRNA. *J. Control. Release.* 2007;1193:360-7.
16. Akita H, Kogure K, Moriguchi R, Nakamura Y, Higashi T, Nakamura T, et al. Reprint of: nanoparticles for ex vivo siRNA delivery to dendritic cells for cancer vaccines: Programmed endosomal escape and dissociation. *J. Control. Release.* 2011;1491:58-64.
17. Toriyabe N, Hayashi Y, Harashima H. The transfection activity of R8-modified nanoparticles and siRNA condensation using pH sensitive stearylated-octahistidine. *Biomaterials.* 2013;344:1337-43.
18. Kusumoto K, Akita H, Ishitsuka T, Matsumoto Y, Nomoto T, Furukawa R, et al. Lipid envelope-type nanoparticle incorporating a multifunctional peptide for systemic siRNA delivery to the pulmonary endothelium. *ACS nano.* 2013; 7:7534-41.
19. Yamada Y, Suzuki R, Harashima H. Investigation of siRNA nanoparticle formation using mono-cationic detergents and its use in gene silencing in human HeLa cells. *Cancers.* 2013;54:1413-25.
20. Futaki S, Ohashi W, Suzuki T, Niwa M, Tanaka S, Ueda K, et al. Stearylated arginine-rich peptides: a new class of transfection systems. *Bioconjug. Chem.* 2001;126:1005-11.
21. Jones LJ, Yue ST, Cheung CY, Singer VL. RNA quantitation by fluorescence-based solution assay: RiboGreen reagent characterization. *Anal. Biochem.* 1998;2652:368-74.
22. Nakase I, Niwa M, Takeuchi T, Sonomura K, Kawabata N, Koike Y, et al. Cellular uptake of arginine-rich peptides: roles for macropinocytosis and actin rearrangement. *Mol. Ther.* 2004;106:1011-22.
23. Khalil IA, Kogure K, Futaki S, Harashima H. High density of octaarginine stimulates macropinocytosis leading to efficient intracellular trafficking for gene expression. *J. Biol. Chem.* 2006;2816:3544-51.
24. Kawamura E, Yamada Y, Yasuzaki Y, Hyodo M, Harashima H. Intracellular observation of nanocarriers modified with a mitochondrial targeting signal peptide. *J. Biosci. Bioeng.* 2013;1165:634-7.
25. El-Sayed A, Khalil IA, Kogure K, Futaki S, Harashima H. Octaarginine- and octalysine-modified nanoparticles have different modes of endosomal escape. *J. Biol. Chem.* 2008;28334:23450-61.
26. Akita H, Kudo A, Minoura A, Yamaguti M, Khalil IA, Moriguchi R, et al. Multi-layered nanoparticles for penetrating the endosome and nuclear membrane via a step-wise membrane fusion process. *Biomaterials.* 2009;3015:2940-9.
27. Lamaze C, Schmid SL. The emergence of clathrin-independent pinocytic pathways. *Curr. Opin. Cell Biol.* 1995;74:573-80.
28. Khalil IA, Kogure K, Akita H, Harashima H. Uptake pathways and subsequent intracellular

trafficking in nonviral gene delivery. *Pharmacol. Rev.* 2006;581:32-45.

29. El Ouaamari A, Baroukh N, Martens GA, Lebrun P, Pipeleers D, van Obberghen E. miR-375 targets 3'-phosphoinositide-dependent protein kinase-1 and regulates glucose-induced biological responses in pancreatic beta-cells. *Diabetes.* 2008;5710:2708-17.

30. Xia HQ, Pan Y, Peng J, Lu GX. Over-expression of miR375 reduces glucose-induced insulin secretion in Nit-1 cells. *Mol. Biol. Rep.* 2011;385:3061-5.

Figure 1. Evaluation of the cellular uptake of R8-LPs using MIN6 and HeLa cells.

A, The cellular uptake of R8-LPs was evaluated by flow cytometry, using MIN6 cells (a) or HeLa cells (b).

The histogram plot shows the fluorescence intensities of R8-LPs labeled with NBD-lipids in cells, at 1 hr after the transduction of R8-LPs (pink lines) and LPs (green lines) (final lipid concentration, 27.5 μ M). Black lines indicate non-treated cells.

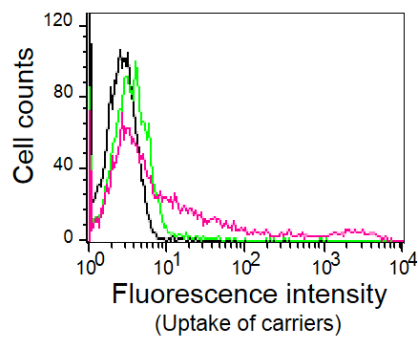
B, Intracellular trafficking of R8-LPs was observed by CLSM, using MIN6 cells (a) or HeLa cells (b). The

carriers labeled with NBD-lipids (green) were incubated in cells for 1 hr (final lipid concentration, 14.2 μ M),

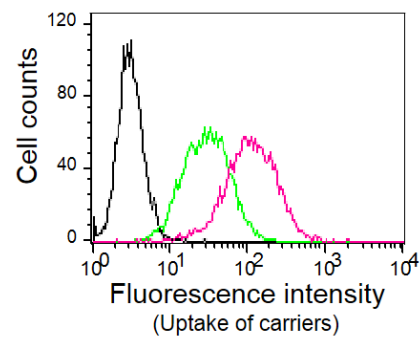
and mitochondria were then stained with TMRM (red) prior to observation. Scale bars, 10 μ m.

A

a. MIN6 cells

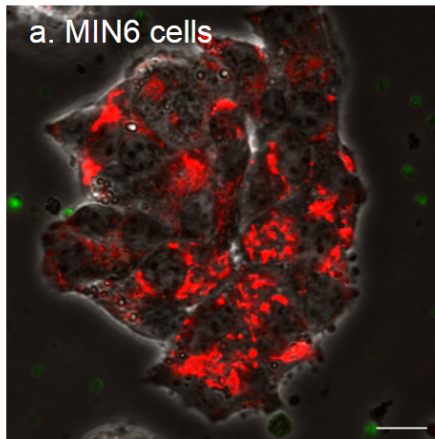


b. HeLa cells



B

a. MIN6 cells



b. HeLa cells

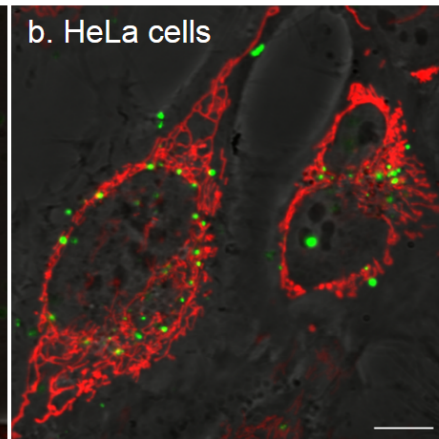


Figure 2. Screening of lipid composition of LPs to efficiently internalize into the MIN6 cells.

The cellular uptake of A-type LP (A), B-type LP (B) and C-type LP (C) was evaluated by flow cytometry, using MIN6 cells (final lipid concentration, 27.5 μ M). The graphs show the mean fluorescence intensity (MFI) of the LPs labeled with NBD-lipids taken up by cells at 1 hr after the transduction of LPs. Data are represented as the mean \pm S.D. (n=3-5). N.D. indicates not detected.

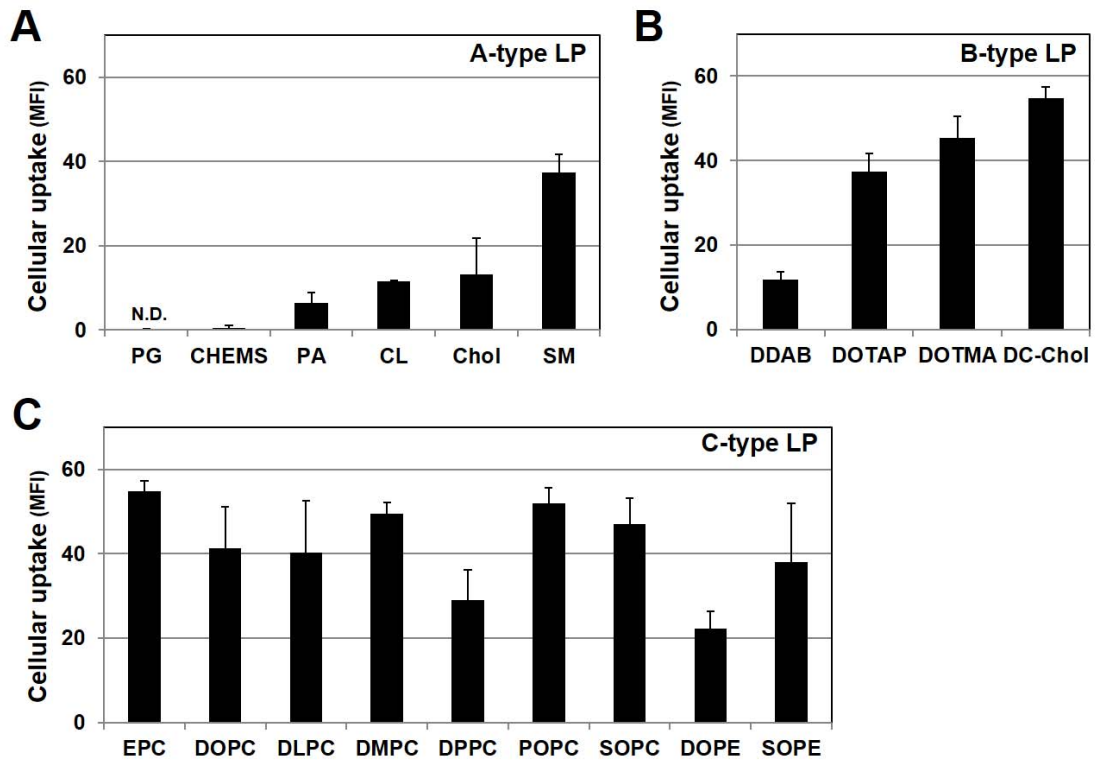


Figure 3. Cellular uptake analysis and intracellular observation of β -MEND in MIN6 cells.

A, The cellular uptake was evaluated by flow cytometry, at 3 hr after transfection of various amounts of Cy5 labelled oligo DNA into MIN6 cells using β -MEND (closed squares), R8-MEND (closed circles) or LFN Plus (closed triangles). MFI, mean fluorescence intensity. Data are represented as the mean \pm S.D. (n=3-6)

*Significant differences ($p < 0.01$) were calculated by one-way ANOVA, followed by Student-Newman-Keuls (SNK) test.

B, Intracellular trafficking of oligo DNA labeled with Cy5 (green pseudo color) was observed by CLSM, at 3 hr after transfection the oligo DNA into MIN6 cells (final oligo DNA concentration, 100 nM), using β -MEND (a), R8-MEND (b) and LFN Plus (c). Non-treated cells were also observed (d). Nuclei were stained with Hoechst33342 (cyan pseudo color) prior to being observed. White lines indicate cell membranes. Scale bars, 10 μ m.

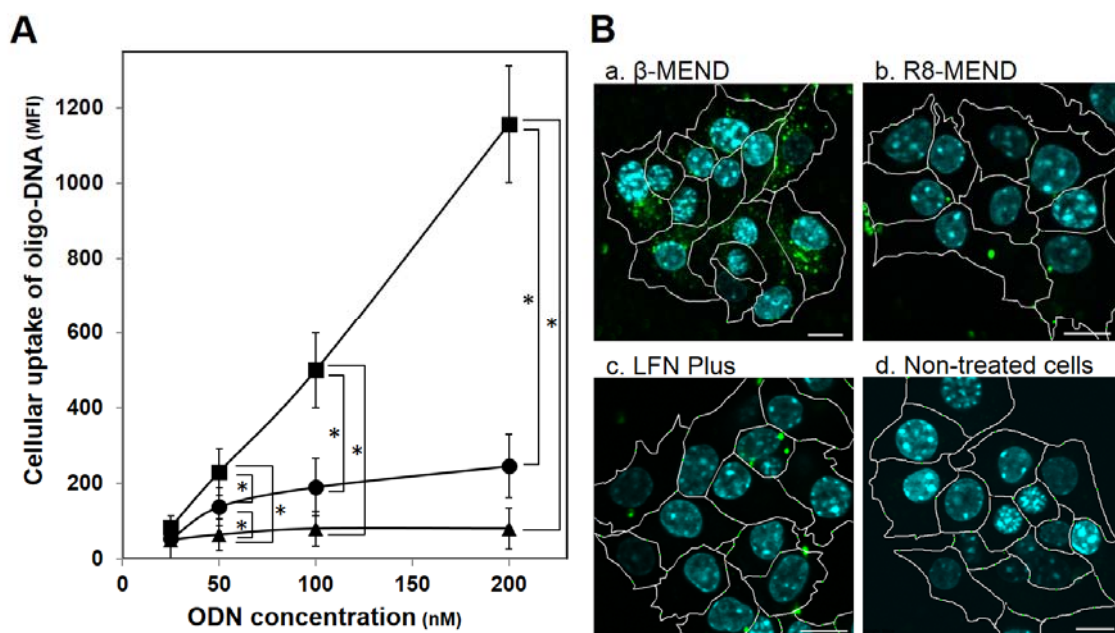


Figure 4. Investigation for the mechanism of cellular uptake using MIN6 cells.

MIN6 cells were incubated with Cy5 labelled oligo DNA encapsulated β -MEND, R8-MEND and LFN Plus (final oligo DNA concentration, 100 nM), in the absence (closed bars) or the presence (open bars) of a hypertonic medium (sucrose, 0.3 M, A), the macropinocytosis inhibitor amiloride (5 mM, B), or the caveolar inhibitor filipin (2 μ g/mL, C). The mean fluorescence intensity (MFI) was measured by flow cytometry at 3 hr after transfection, and is expressed as a percent of the MFI in the absence of inhibitors. Data are represented as the mean \pm S.D. (n=3).

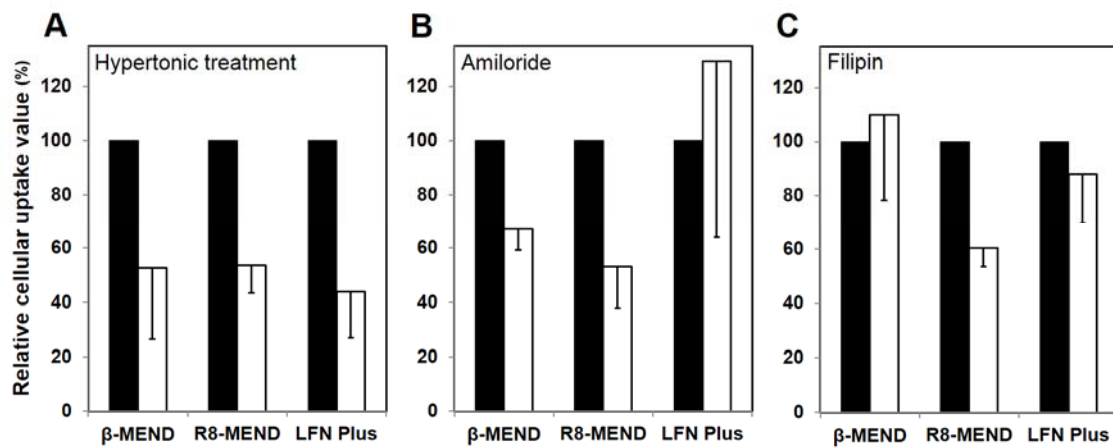


Figure 5. Evaluation of cell viability using MIN6 cells.

Cell viabilities were measured at 24 hr after the transfection of various amounts of oligo DNA, using β -MEND (closed squares), R8-MEND (closed circles) and LFN Plus (closed triangles). Data are represented as the mean \pm S.D. (n=3).

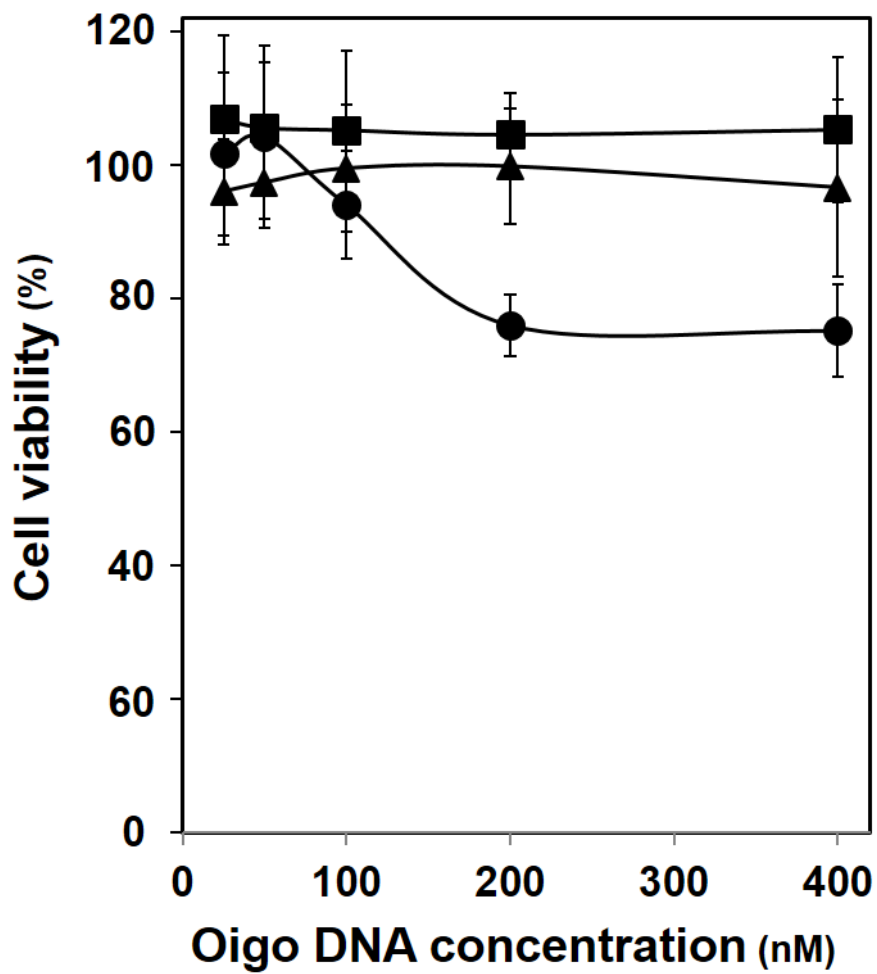


Figure 6. Evaluation of miR-375 knockdown in MIN6 cells by transfection of anti-miR-375 using β -MEND.

MIN6 cells were incubated with anti-miR-375, 2'-OMe RNA complementary to miR375, encapsulated β -MEND (closed squares) or LFN Plus (closed triangles). After 24 hr transfection of carriers, the knockdown effect of miR-375 was evaluated by quantitative RT-PCR. The relative miR-375 expression level indicates a ratio of the miR-375 expression level of the cells treated with anti-miR-375 divided by that of non-treated cells. Data are represented as the mean \pm S.D. (n=3) *Significant difference ($p < 0.01$) was calculated by the two-tail unpaired student's t-test.

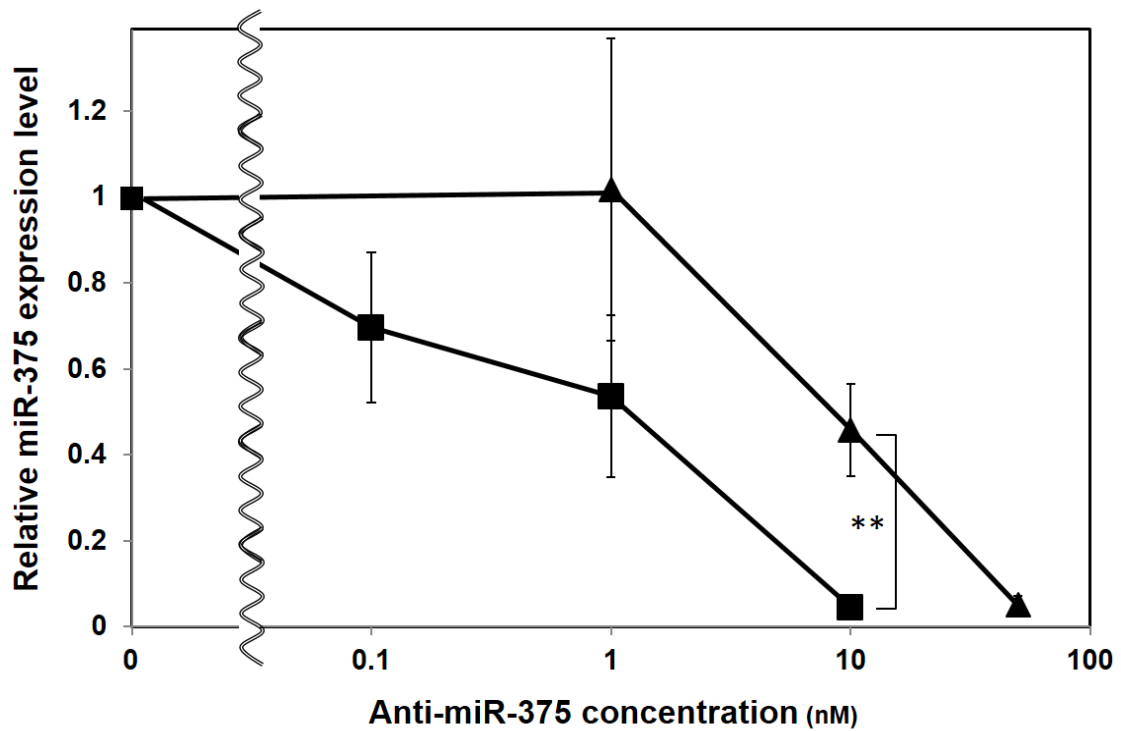


Figure 7. Investigation of insulin secretion after miR-375 knockdown by β -MEND (anti-miR-375) in MIN6 cells.

MIN6 cells were transfected with 2'-OMe RNA complementary to miR-375 (anti-miR-375) at 10, 50, 100 nM with β -MEND (closed bars) or LFN Plus (open bars). Insulin secretion studies were performed at 48 hr after the transfection, and the relative insulin secretion is expressed as a percent of the insulin secretion level of the cells transfected with control RNA. Data are represented as the mean \pm S.D. (n=3-4) *Significant difference ($p < 0.05$) was calculated by the two-tail unpaired student's t-test.

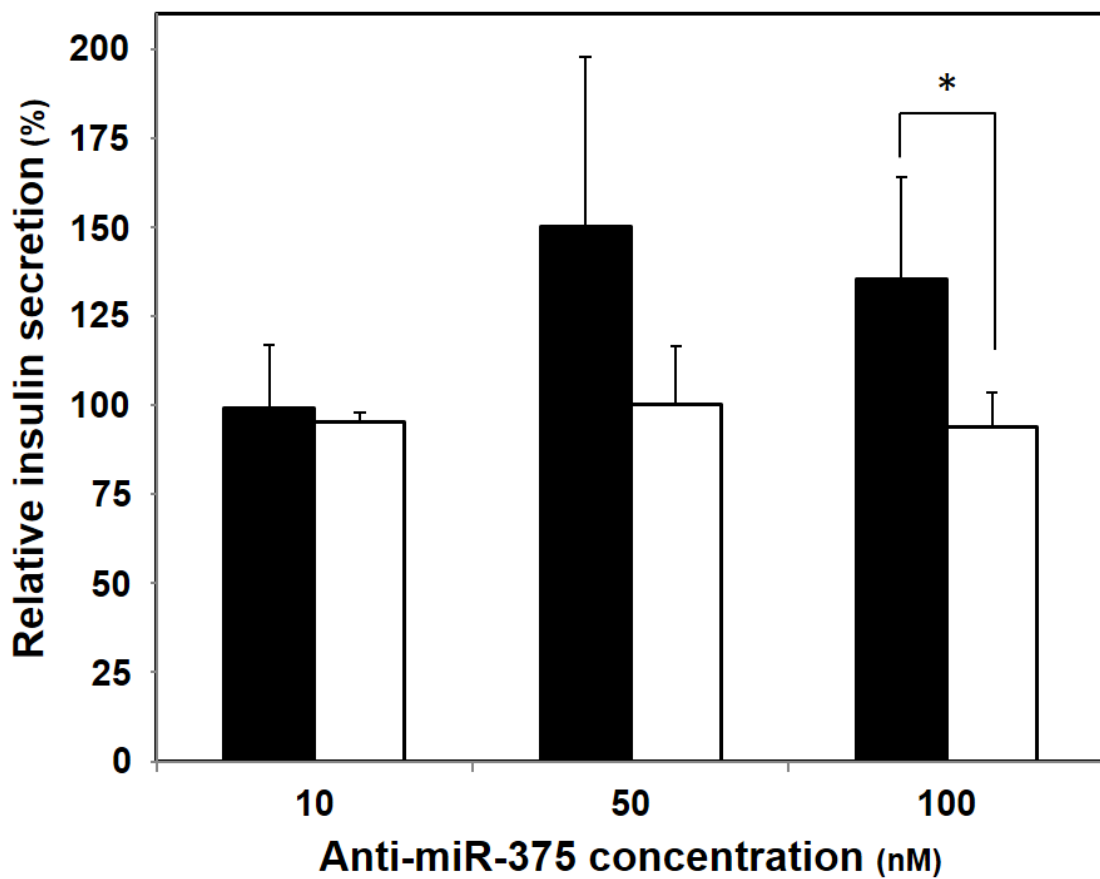


Table 1. Characteristics of LPs.

PG, phosphatidyl glycerol; CHEMS, cholesteryl hemisuccinate; PA, phosphatidic acid; CL, cardiolipin; Chol, cholesterol; SM, sphingomyelin; DDAB, dimethyldioctadecylammonium bromide; DOTAP, 1,2-dioleoyl-3-trimethylammonium-propane; DOTMA, 1,2-di-O-octadecenyl-3-trimethylammonium propane; DC-Chol, 3 β -[N-(N',N'-dimethylaminoethane)-carbamoyl] cholesterol; EPC, egg yolk phosphatidyl choline; DOPC, 1,2-dioleoyl-sn-glycero-3-phosphocholine; DLPC, 1,2-dilawroyl-sn-glycero-3-phosphocholine; DMPC, 1,2-dimyristoyl-sn-glycero-3-phosphocholine; DPPC, 1,2-dipalmitoyl-sn-glycero-3-phosphocholine; POPC, 1-palmitoyl-2-oleoyl-sn-glycero-3-phosphocholine; SOPC, 1-stearoyl-2-oleoyl-sn-glycero-3-phosphocholine; DOPE, 1,2-dioleoyl-sn-glycero-3-phosphoethanolamine; SOPE, 1-stearoyl-2-oleoyl-sn-glycero-3-phosphoethanolamine. Data are represented as the mean \pm S.D. (n=3-5).

Liposome type	Lipid composition	Lipid X	Diameter (nm)	ζ potential (mV)
A-type LP	DOTAP/EPC/Lipid X (3:4:3, molar ratio)	PG	412 \pm 127	-19 \pm 13
		CHEMS	113 \pm 11	-28 \pm 0
		PA	142 \pm 34	-41 \pm 9
		CL	108 \pm 24	29 \pm 10
		Chol	109 \pm 17	39 \pm 8
		SM	92 \pm 3	43 \pm 7
B-type LP	Lipid X/EPC/SM (3:4:3, molar ratio)	DDAB	122 \pm 6	50 \pm 4
		DOTAP	92 \pm 3	43 \pm 7
		DOTMA	119 \pm 17	70 \pm 9
		DC-Chol	102 \pm 6	57 \pm 6
C-type LP	DC-Chol/Lipid X/SM (3:4:3, molar ratio)	EPC	102 \pm 6	57 \pm 6
		DOPC	109 \pm 11	48 \pm 7
		DLPC	107 \pm 17	51 \pm 5
		DMPC	95 \pm 10	51 \pm 11
		DPPC	121 \pm 21	55 \pm 3
		POPC	104 \pm 6	53 \pm 5
		SOPC	110 \pm 10	21 \pm 17
		DOPE	117 \pm 2	43 \pm 4
SOPE	106 \pm 7	58 \pm 5		

Table 2. Characteristics of β -MEND and R8-MEND encapsulating oligo DNA.

PA, phosphatidic acid; SM, sphingomyelin; DC-Chol, 3 β -[N-(N',N'-dimethylaminoethane)-carbonyl] cholesterol; EPC, egg yolk phosphatidyl choline; DOPE, 1,2-dioleoyl-sn-glycero-3-phosphoethanolamine; STR-R8, stearyl octaarginine. Data are represented as the mean \pm S.D. (n=3).

	Lipid composition	Diameter (nm)	ζ potential (mV)	Encapsulation efficiency (%)
β -MEND	DC-Chol/EPC/SM (3:4:3, molar ratio)	235 \pm 25	26 \pm 11	51 \pm 7
R8-MEND	DOPE/PA/STR-R8 (9:2:1, molar ratio)	115 \pm 6	25 \pm 11	51 \pm 5

Supplementary data

1. Materials and Methods

1.1. Investigation of the expression levels of Pdk1 and Mtpn after knockdown of miR-375 by β -MEND system

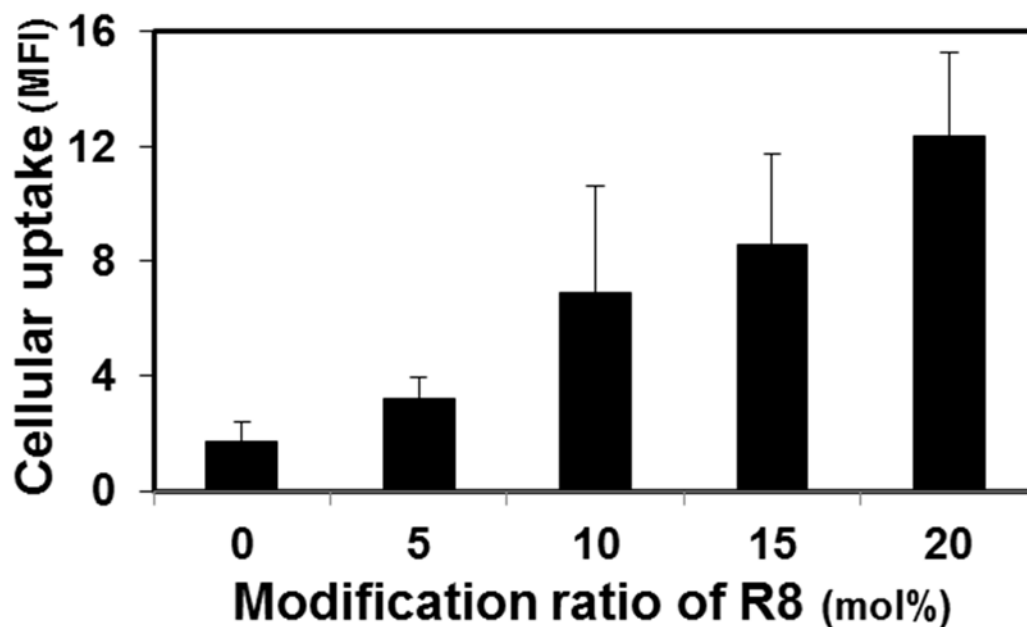
MIN6 cells (4×10^5 cells/mL) were seeded with 5 mL of DMEM containing 10% FBS, on a 60 mm dish (BD Biosciences, Franklin Lakes, NJ, USA). The cells were washed with serum-free DMEM before incubation with the carriers. The carriers containing encapsulated 2'-OMe RNA (anti-miR-375) were added to the cells (final concentration of 2'-OMe RNA, 10 nM), and the cells incubated in serum free DMEM serum under an atmosphere of 5% CO₂ at 37°C. After a 3-hr incubation, the medium was replaced with medium containing serum, and the cells further were incubated for 45 hr.

The cells were then collected and the proteins extracted by suspension in lysis buffer (1% Triton X-100, 50 mM Tris (pH7.5), 200 mM NaCl). The cell lysate was centrifuged (9,000 g, 4°C, 10 min) and the supernatant was collected as the sample for Western blotting. Proteins were separated by 12.5 % sodium dodecyl sulfate-polyacrylamide gel electrophoresis and transferred to a polyvinylidene difluoride membrane. The membrane was blocked by shaking for 1 hr at room temperature in Tris buffered saline with 1% Triton X-100 (TBS-T) containing 5% skim milk. The membrane

was then shaken in a solution of primary antibodies for 1 hr at room temperature in the case of mouse anti-extracellular signal-regulated kinase 1 (Erk1, control protein) antibody derived from rabbit (1:5000, Santa Cruz Biotechnology, Santa Cruz, CA, USA), overnight at 4°C in the case of mouse anti-Pdk1 antibody derived from rabbit (1:500, Cell Signaling, Beverly, MA, USA) and mouse anti-Mtpn antibody derived from rabbit (1:500, Abcom, Cambridge, MA, USA). Anti-Erk1 antibodies and anti-Mtpn antibodies were diluted with TBS-T with 5% skim milk, while anti-Pdk1 antibodies were diluted with Can Get Signal Solution 1 (Toyobo, Osaka, Japan). After washing three times with TBS-T, the membrane was shaken in TBS-T with 5% skim milk containing peroxidase-conjugated secondary anti-rabbit antibody (1:1000, GE Healthcare UK Ltd, England). Detection was performed using Super Signal West Extended Duration Substrate Solution 1 (Thermo Fisher Scientific, Waltham, MA, USA), and immunoreactive bands were visualized using the LAS 4000 (Fujifilm, Tokyo, Japan).

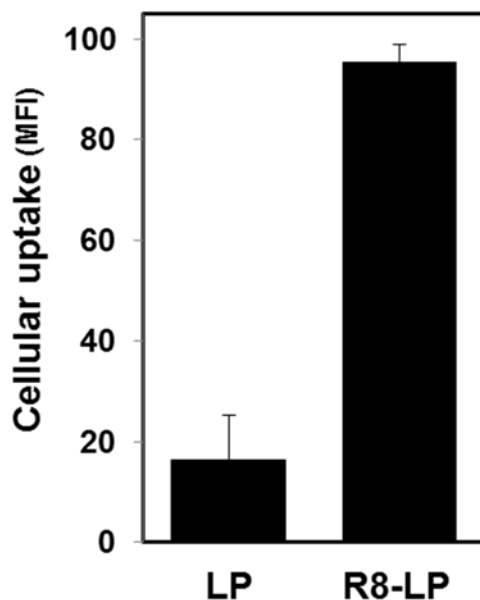
2. Supplementary Figure

Figure S1. Investigation of the cellular uptake of LPs modified with various amounts of R8 in the case of MIN6 cells.



The cellular uptake of R8-modified LPs was evaluated by flow cytometry, using MIN6 cells. In this experiment, the different amounts of R8-modified LPs were used, and their characteristics are summarized in [Table S1](#). The graph shows the mean fluorescence intensity (MFI) of LPs labeled with NBD-lipids that were taken by cells at 1 hr after transduction of LPs. Data are represented as the mean \pm S.D. (n=3).

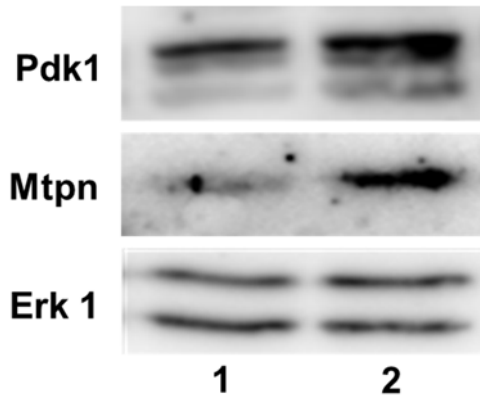
Figure S2. Comparison of the cellular uptake between R8-modified LPs and R8-unmodified LPs using HeLa cells.



Cellular uptakes of 10 mol% of R8 modified LPs (R8-LP) and R8-unmodified LP (LP) were evaluated by flow cytometry, using HeLa cells. The characteristics of R8-LP and LP are summarized in [Table S1](#). The graph shows the mean fluorescence intensity (MFI) of the LPs labeled with NBD-lipids taken up by cells at 1 hr after the transduction of LPs.

Data are represented as the mean \pm S.D. (n=3).

Figure S3. Western blot analysis for the expression levels of Pdk1 and Mtpn in MIN6 cells after transfection of anti-miR-375 by the β -MEND system.



MIN6 cells were treated with β -MEND encapsulating anti-miR-375 (final concentration of 2'OMe-RNA, 10 nM). Western blot analysis was performed at 48 hr after transfection. Each sample (10 μ g of protein) was subjected to western blotting. Primary antibodies against the Pdk1, Mtpn and Erk1 (control) were used. Lane 1, non-treated cells; lane 2, cells treated with anti-miR-375.

3. Supplementary Table

Table S1. Characteristics of LPs modified with different amounts of R8.

Modification ratio of R8 on LP (mol% of total lipids)	Diameter (nm)	ζ potential (mV)
0	125 \pm 9	-53 \pm 11
5	129 \pm 17	-16 \pm 1
10	134 \pm 17	48 \pm 11
15	124 \pm 10	57 \pm 2
20	115 \pm 5	61 \pm 2

The diameters and ζ potentials of LPs (DOPE/PA =9:2) modified with R8 at various molar ratios are summarized. Data are represented as the mean \pm S.D. (n=3-5).